www.amlett.com, www.vbripress.com/aml, DOI: 10.5185/amlett.2015.5649 Published online by the VBRI press in 2015

Tuning of optical properties of glass by embedding silver nanoparticles

Annu Sharma*, Jyoti Rozra, Isha Saini

Department of Physics, Kurukshetra University, Kurukshetra 136 119, India

*Corresponding author. Tel: (+91) 1744 238410 2130; E-mail: talk2annu@gmail.com

Received: 26 November 2014, Revised: 15 January 2015 and Accepted: 28 January 2015

ABSTRACT

In the present work, effects of annealing temperature on structural and optical properties of silver-glass nanocomposites synthesized by the combined use of ion-exchange and subsequent thermal annealing in air have been investigated using Transmission electron microscopy (TEM), UV–Visible absorption spectroscopy and Photoluminescence spectroscopy. The appearance of SPR peak characteristic of silver nanoparticle formation around 429 nm in absorption spectra of silver-glass nanocomposite samples indicates towards the formation of silver nanoparticles in glass. The size of silver nanoparticles has been found to increase with increase in annealing temperature. At an annealing temperature of 200°C the size of silver nanoparticles comes out to be 2.31 nm which increases to a value of 7.60 nm at an annealing temperature of 550°C. TEM investigation indicates that silver nanoparticles of size 6.57±1.14 nm are formed in glass matrix. UV-visible absorption and reflection data has been analyzed to ascertain optical properties such as absorption coefficient (α), refractive index (n) and dielectric constant (ε). Emissions bands in the photoluminescence spectra were analyzed to investigate different oxidation states of silver present in the prepared nanocomposite samples. Formation of Ag^{o} atoms from Ag^{+} ions are responsible for the quenching of photoluminescence intensity at higher temperature. Such nanocomposites are expected to be promising materials for ultrafast optical switches and for sensing applications. Copyright © 2015 VBRI press.

Keywords: Nanocomposites; surface plasmon resonance; refractive index; photoluminescence.

Annu Sharma is working as an Assistant Professor in physics in the Department of Physics, Kurukshetra University, Kurukshetra. Her current research interests include synthesis and characterization of nanocomposite materials; stopping power of heavy ions and effect of ion implantation on the various properties of composite materials She received her PhD degree in Physics in 2001 from Kurukshetra University, Kurukshetra. During 2002to 2004, she worked as an Assistant Professor for post doctoral research with professor Peter Sigmund at Department of Physics, University of Southern Denmark, Odense, Denmark. There are many research publications in the refereed international journals and in symposium and conferences to her credit.

Jyoti Rozra received her B.Sc degree in 2005, M.Sc physics degree in 2007, M.Phil degree in 2009 and Ph.D. in Physics from Kurukshetra University, Kurukshetra India. She is presently studying for her PhD degree in the Department of Physics, Kurukshetra University, Kurukshetra. Her research area includes synthesis and characterization of metal nanoparticle based nanocomposites.

Isha Saini is pursuing her Ph.D. in Physics under supervision of Dr Annu Sharma from Department of Physics, Kurukshetra University, Kurukshetra. She is working in the area of synthesis and characterization of nanocomposites. She has presented around 12 papers in National and International conferences and has received best poster award also. She received her B.Sc degree in 2006, M.Sc physics degree in 2008 and M.Phil degree in 2010 from Kurukshetra University, Kurukshetra India.

Introduction

Nanocomposite materials containing noble metal nanoparticles embedded in glass matrices has recieved special attention due to their notable optical properties owing to the surface plasmon resonance (SPR), the nanoscale feature which is the origin of the observed colors in metal colloids. The SPR arises due to the resonant oscillation of the conduction band electrons when interacting with an external electromagnetic radiation **[1]**. SPR of metal nanoparticles depends on the shape, inter-

particle separation, volume fraction of metal nanoparticles and the dielectric constant of the embedding matrix.

The tunability of the optical properties of these metal-glass nanocomposites makes them suitable for a variety of applications including sensors, color filters and waveguides **[2-3]**. For example, the insertion of silver metal ions in glass matrix gives rise to an intense photoluminescence (PL) emission, which is potentially useful for optoelectronic applications and a simultaneous change in the refractive index is responsible for the fabrication of waveguides **[4-5]**. For such surface plasmon-based applications, it is important to controllably tune the SPR wavelength. Researchers are mainly concentrating on Au and Ag metal nanoparticles because their SPR can be tuned to any desired wavelength in the visible region. Among the metals, silver exhibit highest efficiency of plasmon excitation **[6]**. This property makes silver nanoparticles a proper choice for surface plasmon-based applications. Glass is an excellent host matrix for growing small metal nanoparticles. Moreover, glass matrices provide long-term stability to metal nanoparticles.

Various methods such as low energy ion-beam mixing **[7]**, sol-gel **[8]**, direct metal-ion implantation **[9]**, ion-exchange **[3]**, vacuum deposition **[10]**, field-assisted ion diffusion **[11]** have been reported in the literature for the fabrication of metal doped glass nanocomposites. However ion-exchange method is highly favorable as it is very efficient for introducing very high concentrations of metal ions into the glass matrix and simultaneously keeping it intact, besides being economical. In literature, there are numerous reports on the synthesis of silver metal nanoparticles in glass by ion-exchange method followed by ion-irradiation **[12]**, annealing in reduced atmosphere **[13]** or in a high vacuum atmosphere **[14]**.

However, there are only a few reports where annealing has been carried in air but at very high temperatures and for long durations **[15]**. Several authors have reported the vanishing of SPR peak of silver nanoparticles when annealing has been carried out in air and ascribed it to oxidation of nanoparticles **[16]**. This oxidation of silver nanoparticles leading to formation of silver oxides is responsible for the instability in plasmonic response, which limits the practical applications of silver-glass nanocomposites. Besides this, there is dearth of reports describing important properties like reflection, transmission, refractive index, real and imaginary part of dielectric constant, photoluminescence of such nanocomposites. Thus a comprehensive characterization capable of exploring the optical properties of such nanocomposites as a function of annealing temperature is important from both fundamental and technological point of views. Until now there is no reliable and universal method to give a conclusive explanation to observed features, however optical absorption and photoluminescence spectroscopy have proved to be valuable tools in studying the evolution of the optical properties of silver-glass nanocomposites as a function of annealing temperature **[14]**.

The aim of the presented work was to demonstrate a binary ion-exchange technique followed by thermal annealing for the fabrication of metal-glass nanocomposites in which silver nanoparticles of various sizes were incorporated inside the glass matrix. Such nanocomposites can be used as promising materials for novel functional applications in plasmonics and photonics. The optical properties such as refractive index, extinction coefficient and dielectric constant of the nanocomposites before and after annealing were studied by optical absorption spectroscopy and luminescence behavior was studied using photoluminescence spectroscopy. Heat treatment induced changes observed in photoluminescence intensity have been correlated to the growth of silver nanoparticles.

Experimental

Materials

All chemicals used were of analytical reagent grade and were used as received. The $AgNO_3$ and $NaNO_3$ were purchased from Rankem. Commercially available glass slides of dimensions (75mm×25mm×1.3mm) and (composition (in wt%) 71.86% SiO_2, 13.30% Na_2O, 8.69% CaO, 4.15% MgO, 1.92% Al_2O_3, 0.08% Fe_2O_3) supplied by (Polar Industrial Corporation, Mumbai, India) were used as substrates. First the substrates were washed with distilled water and further cleaned with extra-pure acetone (99.5% purity) in order to remove surface contaminants. Subsequently, they were rinsed with distilled water and dried.

Synthesis of nanocomposites

Silver ion-exchanged glass samples were prepared by immersing the preheated glass slides for 1 min in a molten salt bath of $AgNO_3$ and $NaNO_3$ (1:4 weight ratio) mixture at the temperature of 350°C. The obtained silver exchanged glass samples were rinsed with distilled water to remove excess $AgNO_3$ adhering on glass surface. Subsequently, these silver ion-exchanged samples were annealed in air at various temperatures from 200°C to 550°C for 1 hour. The resulting silver ion-exchanged glass samples annealed at various temperatures were utilized for further characterization.

To determine the size of the silver nanoparticles embedded in glass matrix, TEM measurements were performed using a Hitachi "H-7500" transmission electron microscope operated at accelerating voltage of 80 kV. For sample preparation, a diamond scriber was utilized to scratch the surface (a few microns below) of the glass containing silver nanoparticles. Minute powder thus obtained was dropped in the methanol and kept for ultrasonification for about 20 minutes. Due to agitation larger glass particles settled down and the finer ones floated on the surface of the liquid. Subsequently, the finest layer on the surface was collected on a carbon coated copper grid for observation.

The reflection and absorption spectra of silver-glass nanocomposite samples were recorded using Shimadzu Double Beam Double Monochromator Spectrophotometer (UV-2550) equipped with an Integrating Sphere Assembly ISR-240A in the wavelength range of 190 nm to 900 nm with a resolution of 0.5 nm. For recording diffuse reflection spectra, $BaSO_4$ powder was taken as the reference material whereas for recording absorption spectra air was used as reference. From these spectra, optical constants such as refractive index, extinction coefficient, real and imaginary

part of dielectric constant were determined. Photoluminescence measurements of nanocomposite samples were carried out at different excitation wavelength range from 270-370 nm using Jobin Yvon Spectroflurometer (Spex FluoroMax-3) where Xenon lamp was employed as the excitation source. All emission spectra were recorded by mounting the samples in solid sample holder (model 1933) at an angle of 30°with a resolution of 1 nm.

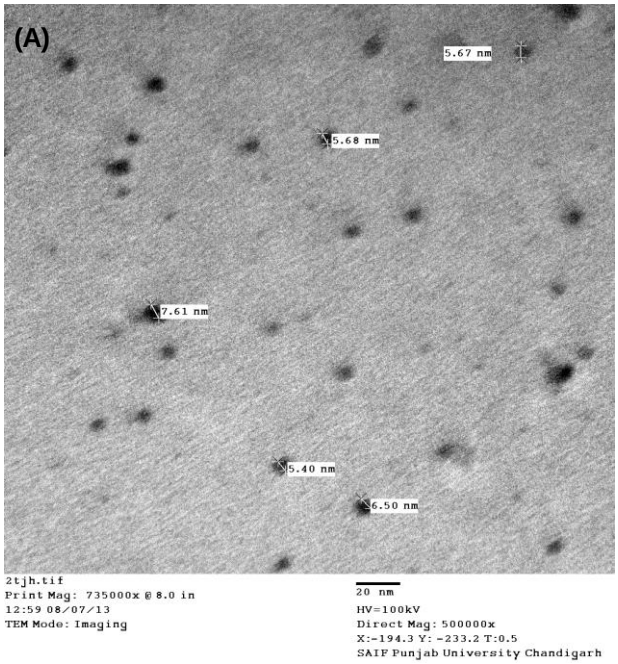

Fig. 1. (A) TEM micrograph of the silver nanoparticles in the ion-exchanged glass sample annealed at 550°C and (B) Size distribution of silver nanoparticles.

Results and discussion

TEM measurements

Fig. 1(A) shows the TEM micrograph of silver ion-exchanged glass sample annealed at 550°C and **Fig. 1(B)** shows the size distribution of silver nanoparticles as obtained from TEM image. TEM micrograph indicates that spherical silver nanoparticles of size 6.57±1.14 nm are well dispersed inside the glass matrix with adequate spacing.

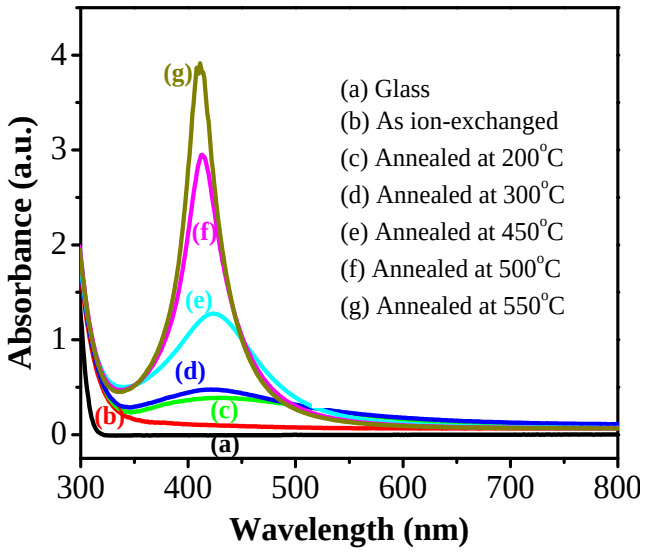

Fig. 2. Optical absorption spectra of (a) glass (b) silver exchanged glass and annealed at (c) 200°C (d) 300°C (e) 450°C (f) 500°C and (g) 550°C.

UV-visible absorption

The UV-Visible absorption spectra for silver exchanged glass samples before and after thermal annealing in air at various temperatures (200°C to 550°C) are shown in **Fig. 2.** Prior to the ion-exchange process, the glass samples were colourless and had no measurable absorption in the visible region [**Fig. 2 curve (a)**]. No obvious SPR peak characteristic of silver nanoparticles (400–430 nm) **[1]** formation was observed in silver ion-exchanged glass sample before annealing [**Fig. 2 curve (b)**]. Absence of SPR absorption peak in silver ion-exchanged glass sample indicates that the volume fraction of silver nanoparticles is very low and silver mainly exist in Ag^+ form. However, at an annealing temperature of 200°C [**Fig. 2 curve (c)**] a wide SPR absorption band starts appearing, centered at about ~429 nm **[17]**. Appearance of a broad and week band at an annealing temperature of 200°C indicates that with increasing temperature a part of Ag^+ ions are being converted into neutral silver atoms and further these atoms nucleate and grow into silver nanoparticles. The width of the observed SPR peak might also be due to the size distribution of silver nanoparticles in glass matrix. When the silver ion-exchanged glass samples were annealed at 300°C and 450°C, the SPR peak becomes narrow and the absorption intensity increases [**Fig. 2 curves (d)** and **(e)**]. With the further increase in annealing temperature to 500°C and 550°C [**Fig. 2 curves (f)** and **(g)**] SPR peak becomes significantly narrow and absorption intensity increases further.

The observed substantial increase in absorption intensity and narrowing of the full width at half maxima (FWHM) of the absorption peak with increasing annealing temperature can be ascribed to an increase in volume fraction and size of silver nanoparticles in the glass matrix **[18]**. The appearance of nearly symmetrical absorption

peaks at various annealing temperatures [**Fig. 2 curves (e), (f) and (g)**] indicate towards the formation of spherical silver nanoparticles inside the glass matrix. Moreover, the colour of the transparent glass samples changes from colourless to light yellow, at an annealing temperature of 200°C, which is a characteristic of silver nanoparticles formation. With the increasing annealing temperature the intensity of yellow colour also increases.

From absorption spectra, size of silver nanoparticles was calculated using the following formula, assuming the free particle behaviour of the conduction electron **[10]**:

$$d = \frac{hv_f}{\pi \Delta E_{1/2}} \quad (1)$$

where d is the diameter of the nanoparticles, V_f (1.39×10^6 m/sec) is the Fermi velocity of electrons in bulk silver, $h=2\pi\hbar$ is the Planck's constant and ΔE is the FWHM of the absorption band. The above equation is valid as long as the dimension of silver nanoparticles is smaller than the mean free path of the electrons in the bulk metal **[1]**. The mean free path of electrons is about 27 nm at room temperature for bulk silver.

Annealing temperature, SPR peak position, FWHM and diameter of silver nanoparticles embedded in glass are listed in **Table 1**. The size of silver nanoparticles calculated using Eq. (1), at an annealing temperature of 200°C comes out to be around 2.31 nm which increases to a value of 7.60 nm at an annealing temperature of 550°C is shown in **Table 1**. The size calculated using UV-Visible absorption spectra agrees fairly well with the size determined using TEM.

Table 1. Annealing temperature, SPR peak position, FWHM and diameter of the silver nanoparticles embedded in soda glass.

Annealing Temp (°C)	SPR peak (nm)	FWHM (nm)	Diameter d (nm)
200	429.6	0.79	2.31
300	423.9	0.65	2.80
450	423.8	0.47	3.89
500	412.9	0.27	6.76
550	410.8	0.24	7.60

In the ion-exchange process at 350°C, Na^+ ions (ionic radius=0.96 Å) present in the glass are replaced by the larger Ag^+ ions (ionic radius=1.26 Å) from the molten salt **[19]**. This reaction can be represented by Eq. (2):

$$\equiv Si-O-Na^{1+} + Ag^{1+}NO_3^- \rightarrow \equiv Si-O-Ag^{1+} + Na^{1+}NO_3^- \quad (2)$$

As a result the size of free volume inside the host matrix decreases and consequently its electron density increases. The silver atoms in ion-exchanged glass mainly exist as Ag^+ ions along with a small fraction of Ag^o atoms. When silver ion-exchanged glass samples are annealed, Ag^+ ions induced by a diffusion process are reduced to silver (Ag^o) atoms by capturing the electrons from the glass matrix. The Ag^o atoms are mainly bound to the non-bridging oxygen (NBO) atoms in glass matrix. During annealing Ag–O bonds break forming more Si–O and Ag–Ag bond and hence neutral Ag^o atoms become the dominant state. The mechanism of Ag^o atoms formation eventually leading to silver nanoparticle formation and can be represented by the following reactions **[20]**:

$$2(\equiv Si - O^- Ag^+) \leftrightarrow \equiv Si-O-Si\equiv + O^{1-} + (Ag_2)^{1+} \quad (3)$$

$$2O^{1-} + 2Ag^{1+} \leftrightarrow 2Ag^{\circ} + O_2 \quad (4)$$

From Eq. (4) it is clear that with increasing annealing there is an enhancement in the reduction of Ag^+ ions to Ag^o atoms, which leads to an increase in the concentration of the mixed (Ag^++Ag^o) silver species. Thus the increasing size of silver nanoparticles with increasing annealing temperature may be attributed to the aggregation of silver nanoparticles by diffusion.

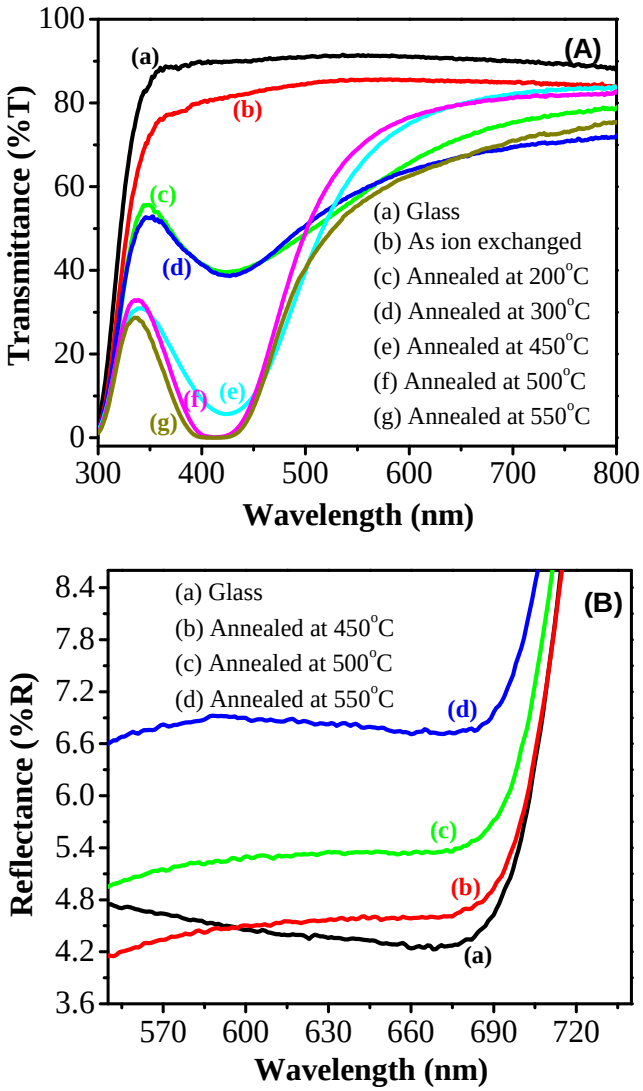

Fig. 3. (A) Transmission spectra of glass and silver-glass nanocomposite samples and (B) Reflection spectra of glass and silver-glass nanocomposite samples.

Further, it can be discerned from **Table 1** that with increasing annealing temperature, besides the increase in size of silver nanoparticles a blue shift in SPR peak position is also observed. This blue shift in SPR peak position can be attributed to the boundary coupling (interface interaction) between silver nanoparticles and glass matrix. The interactions at the surface of silver nanoparticles may be due to their high activity, and during these interface interaction charge transfer occurs from silver nanoparticles to the glass matrix. Due to this charge transfer the free electron density of silver nanoparticles decreases which gives rise to a blue shift in the absorbance peak with the increasing size of silver nanoparticles. Similar explanation for blue shift of SPR peak with increasing size of nanoparticle has been reported for gold nanoparticles in gold-alumina composite film **[21]** and also for silver nanoparticles dispersed within the glass matrix **[22]**.

Fig. 3 shows optical transmission and reflection spectra of glass and silver ion-exchanged glass samples annealed at various temperatures as a function of wavelength. All transmission spectra display a transmission cut-off below 300 nm due to the absorption of the glass substrate. It can be clearly discerned from **Fig. 3** [**curve (a)]** for soda glass, the transmission is maximum nearly 90% in the whole visible region (400-700 nm). This clearly supports the transparency of soda glass. As can be seen in **Fig. 3**, ion-exchange causes a slight decrease in transmission over the entire spectral range, the reason behind this can be the substitution of sodium ions by silver ions, which decreases light transmission and increases light absorption. At an annealing temperature to 450°C **[curve (e), Fig. 3]** a transmission dip evolves, centered at λ=~429 nm which is generally attributed to the surface plasmon resonance of silver nanoparticles embedded in glass matrix. At highest annealing temperature of 550°C **[curve (g), Fig. 3]** the transmission decreases to 0.2% at a wavelength ~410 nm. Thus, it is clear from **Fig. 3** that the transmission and reflection coefficient decreases while the absorbance coefficient, on the contrary increases, with increasing annealing temperature. This sharp fall in transmittance can be of potential use as long-wavelength pass filters in integrated optics, where the cutoff wavelength can be adjusted via the length of the region containing silver nanoparticles.

The optical absorption and reflection data was further analyzed to determine the optical constants of silver-glass nanocomposite samples. The complex refractive index (n*=n-ik) and dielectric function characterize the optical properties of any solid materials. The real part of the refractive index, n, gives the dispersion and the imaginary part of the refractive index, k, gives the absorption of the electromagnetic wave. The knowledge of refractive index (n) is an essential input parameter to obtain the required index-matching in waveguide applications of such composites.

The extinction coefficient k in the entire visible region for glass and silver ion-exchanged glass samples annealed at various temperatures has been calculated from the absorption spectra **(Fig. 2)** using the relation given below **[23]**:

$$k = \frac{\alpha\lambda}{4\pi} \quad (5)$$

where α is the optical density and λ is the wavelength of the light used.

Refractive index (n) of the glass and silver ion-exchanged glass samples, annealed at various temperatures has been calculated from the reflectance and extinction coefficient values by using the following relation **[24]**:

$$R = \frac{(n-1)^2 + k^2}{(n+1)^2 + k^2} \quad (6)$$

Solving Eq. (6) for refractive index (n) gives.

$$n = \frac{(1+R) + \sqrt{4R - (1-R)^2 k^2}}{(1-R)} \quad (7)$$

where R is the reflectance.

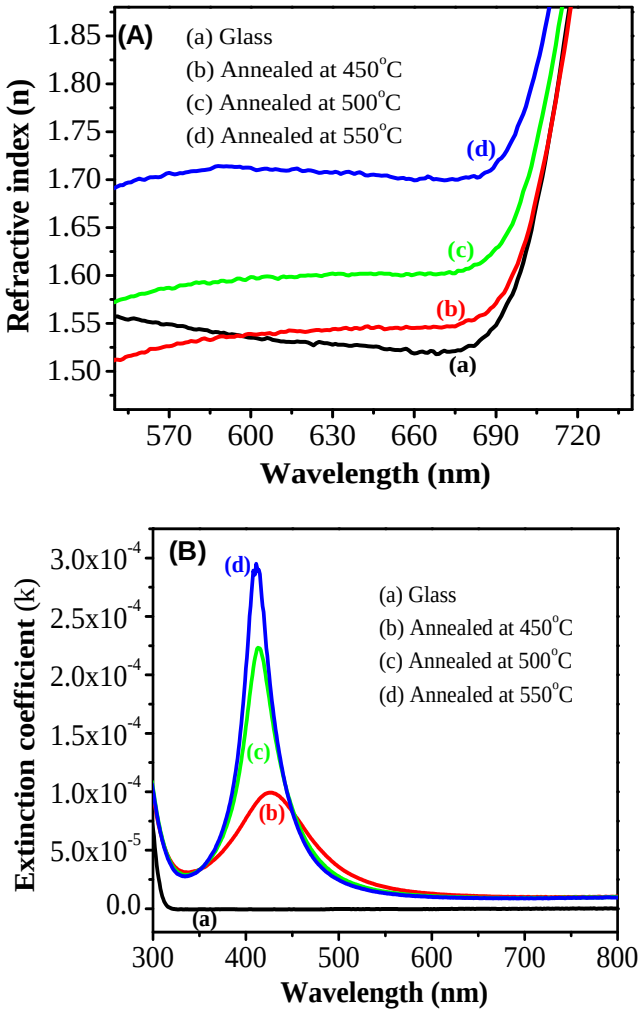

Fig. 4. (A) Variation of refractive index (n) with wavelength for glass and silver-glass nanocomposite and (B) Variation of extinction coefficient (k) with wavelength for glass and silver-glass nanocomposites.

The variation of extinction coefficient and refractive index of prepared silver-glass nanocomposite samples with wavelength are shown in **Fig. 4**. It is clear from **Fig. 4** that

the values of extinction coefficient and refractive index increases with increasing annealing temperatures.

It can be discerned from **Fig. 4** that the refractive index that was measured at visible wavelengths became more pronounced for silver nanoparticles embedded glass samples as compared to glass. The value of refractive index for soda glass **[curve (a), Fig. 4]** is 1.52 at a wavelength of 600 nm. At an annealing temperature of 550°C, value of refractive index of silver-glass nanocomposite sample increase to 1.71 due to incorporation of silver nanoparticles of size 6.57±1.14 nm in glass. The large value of n and k indicate that the resulting silver-glass nanocomposite is absorbing the light. As the size and volume fraction of the silver nanoparticles increases in soda glass matrix the refractive index of the nanocomposite samples increase. The cause of alteration in the refractive indices may be due to the structural changes and volume variations taking place during the ion-exchange process.

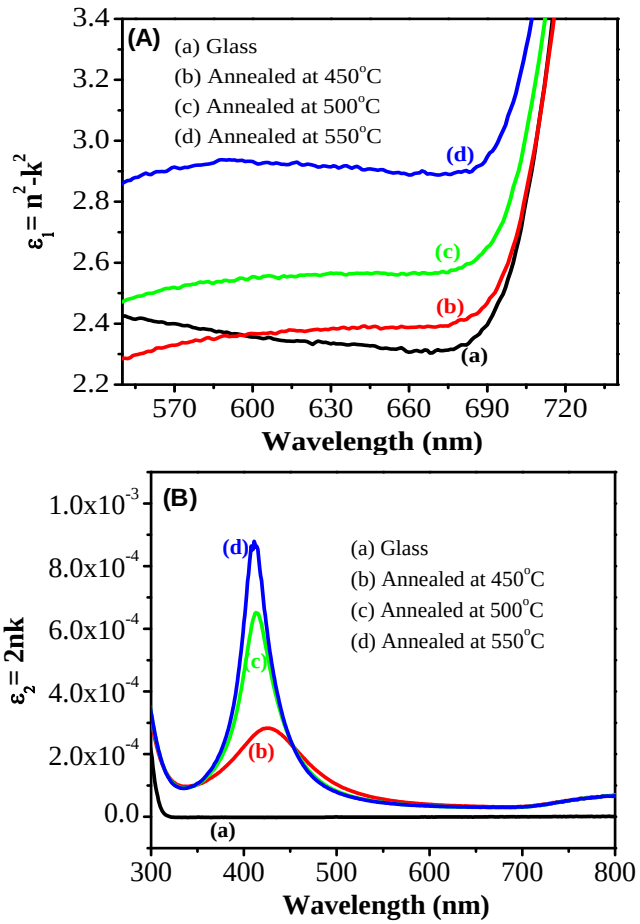

Fig. 5. (A) Variation of real part of dielectric constant with wavelength for glass and silver-glass nanocomposite samples and (B) Variation of imaginary part of dielectric constant with wavelength for glass and silver-glass nanocomposite samples.

The obtained refractive index data was further analyzed to obtain the real and imaginary part of dielectric constant. In optics, the real part of dielectric constant is closely related to the refractive index and the imaginary part is to the extinction coefficient which represents the losses of photon energy when optical wave propagates through the media. The real and imaginary part dielectric constant was determined by the following relations **[25]**.

$$\varepsilon_1 = n^2 - k^2 \quad (8)$$

$$\varepsilon_2 = 2nk \quad (9)$$

The variation of real and imaginary parts of the dielectric constant with wavelength calculated using Eqs. (8) and (9) of glass and silver-glass nanocomposite samples are shown in **Fig. 5**.

As the particle size is in nanometer range, the number of particles per unit volume is large; hence the dipole moment per unit volume increases, and so the dielectric constant increases. A significant increase in the value of real part of dielectric constant at wavelength 550 nm from 2.4 for glass to 2.9 for silver ion-exchanged glass nanocomposite formed after annealing at 550°C was observed. Thus with the insertion of silver nanoparticles of size 6.57±1.14 nm in glass the dielectric constant of resulting nanocomposite increases drastically. The values of the real part of dielectric constant are higher than the imaginary part. In relevance to light, the real part of the dielectric constant represents the degree to which a material can be polarized by an external electromagnetic field and the imaginary part represents optical losses such as absorption due to inter-band transitions and inelastic electron phonon/electron-electron interactions. Therefore, we can conclude that the energy storage capacity of prepared nanocomposites is high because of large value of real part of dielectric constant.

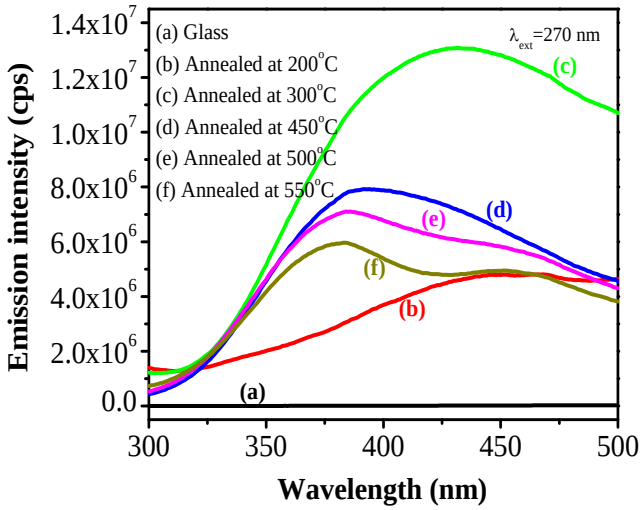

Fig. 6. Photoluminescence spectra of (a) glass, silver ion-exchanged glass samples annealed at temperatures (b) 200°C (c) 300°C (d) 450°C (e) 500°C and (f) 550°C excited at an excitation wavelength of 270 nm.

Photoluminescence spectroscopy

Fig. 6 shows the photoluminescence (PL) spectra of glass and silver-glass nanocomposite samples annealed at different temperatures. At the excitation wavelength of 270 nm, silver ion-exchanged samples annealed at 200°C and 300°C show a broad emission band centered around 454 and 434 nm respectively. Sample annealed at 450°C show a blue shifted intense broad emission band centered at around 400 nm. Sample annealed at 500°C again show two intense broad emission bands centered at around 385

nm and 460 nm. When the annealing temperature is further increased to 550°C the two bands are shifted to 381 nm and 453 nm respectively, however these bands are less intense than the bands observed in the samples annealed at 300°C and 450°C. It is well known **[26]** that the presence of Ag^+ in glass matrices is responsible for characteristic PL emissions in the visible range, after electronic excitation between the $4d^{10}$ ground state to some levels of the $4d^95s^1$ silver ion configuration. Although, these transitions are parity-forbidden, they are partially allowed in a solid due to vibrational coupling.The ground state of free silver ion is $^1S_0$ and the excited state of free silver ion is split into number of energy states $^3D_3$, $^3D_2$, $^3D_1$ and $^1D_2$ (Russell-Saunders statesarising from $4d^95s^1$ Ag^+ configuration) in increasing order of energy **[27]**. Thus it is resonable to assign the emission band observed at 454 nm for sample annealed at 200°C to spin-forbidden transitions from ^3D_j states to $^1S_0$ states. Further, emission band displayed at lower wavelength 434 nm for sample annealed at 300°C can be assigned to spin allowed transitions from the $^1D_2$ state to the ground $^1S_0$ state. Similarly, for samples annealed at 500°C and 550°C, emission band observed at lower wavelength can be ascribed to spin allowed transitions from the $^1D_2$ state to the ground $^1S_0$ state and the emission bands appearing at higher wavelength can be assigned to spin-forbidden transitions from ^3D_j states to $^1S_0$ states. Furthermore, PL intensity is maximum at the annealing temperature of 300°C, but when temperature is increased further from 450°C to 550°C PL intensity decreases. It is well established **[28]** that Ag^+ ions are luminescent in nature in both crystalline and glassy matrices**.** In view of this, we can say that increase in PL intensity at an annealing temperature of 300°C could be due to the increase of volume fraction of Ag^+ in the bulk of the glass matrix and the drastic decrease in PL intensity with further increase in annealing temperature can be due to the conversion of Ag^+ to Ag^o. This observation correlates well, with the UV-Visible absorption measurements. Conversion of Ag^+ ions to Ag^o atoms is responsible for the increase in absorption intensity with increase in annealing temperature to 550°C as observed in UV-Visible spectra and depicted in **Fig. 2**. Hence increase in annealing temperature from 300°C to 550°C leads to the swift growth of silver nanoparticles and that might have resulted in the diminishing of PL intensity.

Further the dependence of PL spectra on excitation wavelength has been studied. **Fig. 7** shows effect of different excitation wavelengths in the wavelength range of 270-370 nm on PL spectra of silver ion-exchanged glass samples annealed at 300°C as they show maximum PL intensity. From **Fig. 7** it is clear that with increasing excitation wavelength from 270-370 nm, a red-shift in emission band occur. At an excitation wavelength of 270 nm, deep-blue emission band is observed at 434 nm. This band may be attributed to Ag^+ ions **[29]** present in silver-glass nanocomposite samples. At excitation with 320 nm a green emission band is observed at about 530 nm and this may be attributed to Ag^+-Ag^+ pairs **[29]**. Emission band observed at 556 nm at an excitation wavelength of 370 nm may be due to presence of Ag^+ ions and their complexes **[30]**. The emission spectrum of nanocomposite samples also shows a slight dip at~ 410 nm which can be ascribed to surface plasmon absorption of silver nanoparticles. Thus PL spectra of silver doped glasses measured at different excitation wavelengths can successfully reveal that silver could be in different oxidation states in the silver ion-exchanged glass samples and this charge state of silver plays an important role in determining the optical properties of such nanocomposites.

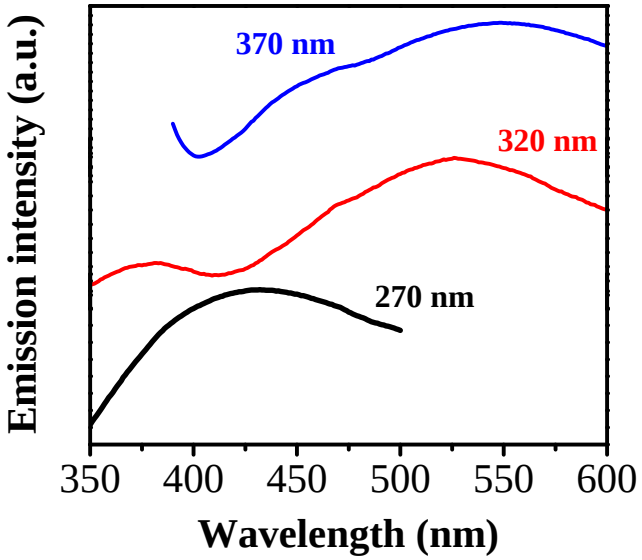

Fig. 7. Photoluminescence spectra for silver ion-exchanged glass sample annealed at 300°C at different excitation wavelengths.

Conclusion

In conclusion, we have discussed the optical and structural properties of silver-glass nanocomposites prepared via ion-exchange method followed by thermal annealing in air. The appearance of surface plasmon resonance peak nearly at ~429 nm in the optical absorption spectra of silver ion-exchanged glass sample annealed at 200°C confirm the formation of silver nanoparticles. At an annealing temperature of 200°C, Ag^+ ions reduce to Ag^o atoms and subsequently at higher annealing temperature Ag^o atoms aggregate to form silver nanoparticles even in air. Size of the silver nanoparticles in glass was found to be 7.60 nm (at 550°C) which agrees well with transmission electron microscopy. Increase in the value of refractive index and dielectric constant of silver-glass nanocomposites may be ascribed to the insertion of silver nanoparticles inside the glass matrix. Analysis of photoluminescence spectra indicate that observed emission band is due to transitions from ^3D_j states to $^1S_0$ states of Ag^+ ions. Such studies are vital to exploit their potential applications in opto-electronic devices.

Reference

1. Keirbeg, U.; Vollmer, M. *Optical Properties of Metal Cluster*, Springer, New York, **1995**.
2. Stalmashonak, A.; Seifert, G.; Abdolvand, A. *Ultra-Short Pulsed Laser Engineered Metal-Glass Nanocomposites*, Verlag: Springer, **2013**.
DOI: 10.1007/978-3-319-00437-2
3. Mohapatra, S. *J. Alloys Comp.* **2014**, *598*, 11.
DOI: 10.1016/j.jallcom.2014.02.021

4. Venkateswara Rao, G.; Shashikala, H. D. *J. Non-Cryst. Solids* **2014**, *402*, 204. **DOI:** 10.1016/j.jnoncrysol.2014.06.007
5. Oven, R. *Appl. Opt.* **2011**, *50*, 5073. **DOI:** 10.1364/AO.50.005073
6. Evanoff, D. D.; Chumanov, G. *Chemphyschem* **2005**, *6*, 1221. **DOI:** 10.1002/cphc.200500113
7. Gangopadhyay, P.; Kesavamoorthy, R.; Nair, K. G. M.; Dhandapani, R. *J. Appl. Phys.* **2000,** *88*, 4975. **DOI:** 10.1063/1.1290739
8. Epifani, M.; Giannini, C.; Tapfer, L.; Vasanelli, L. *J. Am. Ceram. Soc.* **2000**, *83*, 2385. **DOI:** 10.1111/j.1151-2916.2000.tb01566.x
9. Xiao, X. H.; Dong, W.; Wu, W.; Peng, T. C.; Zhou, X. D.; Ren, F.; Jiang, C. Z. *J. Nanosci. Nanotechnol.* **2010,** *10*, 6424. **DOI:** 10.1166/jnn.2010.2528
10. Rozra, J.; Saini, I.; Aggarwal, S.; Sharma, A. *Adv. Mat. Lett.* **2013**, *4*, 598. **DOI:** 10.5185/amlett.2013.1402
11. Sancho-Parramon, J.; Janicki, V.; Dubcek, P.; Karlusic, M.; Gracin, D.; Jaksic, M.; Bernstorff, S.; Meljanac, D.; Juraic, K. *Opt. Mater.* **2010**, *32*, 510. **DOI:** 10.1016/j.optmat.2009.11.004
12. Mahnke, H. E.; Zizak, I.; Schubert-Bischoff, P.; Koteski, V. *Mater. Sci. Eng. B* **2008**, *149*, 200. **DOI:** 10.1016/j.mseb.2007.11.036
13. Borsella, E.; Cattaruzza, E.; Marchi, GDe.; Gonella, F.; Mattei, G.; Mazzoldi, P.; Quaranta, A.; Battaglin, G.; Polloni, R. *J. Non-Cryst. Solids* **1999**, *245*, 122. **DOI:** 10.1016/S0022-3093(98)00878-3
14. Gangopadhyay, P.; Kesavamoorthy, R.; Bera, S.; Magudapadhy, P.; Panigrahi, B. K.; Narasimhan, S. V. *Phys. Rev. Lett.* **2005,** *94*, 047403. **DOI:** 10.1103/PhysRevLett.94.047403
15. Sheng, J. *Int. J. Hydrogen Energy* **2009**, *34*, 2471. **DOI:** 10.1016/j.ijhydene.2009.01.034
16. Hu, J.; Cai, W.; Zeng, H.; Li, C.; Sun, F. *J. Phys.: Condens. Matter* **2006**, *18*, 5415. **DOI:** 10.1088/0953-8984/18/23/013
17. Manikandan, P.; Manikandan, D.; Manikandan, E.; Ferdinand, A. C. Spectrochim, Acta Part A: Mol. Biomol. Spectros. **2014**, *124*, 203. **DOI:** 10.1016/j.saa.2014.01.033
18. Udayabhaskar, R.; Karthikeyan, B.; Ollakkan, M. S.; Mangalaraja, R. V.; Baesso, M. L. *Chem. Phys. Lett*. **2014**, *593*, 1. **DOI:** 10.1016/j.cplett.2013.12.058
19. Shaaban, M. H.; Mahmoud, K. R.; Sharshar, T.; Ahmed, A. A. *Nucl. Instr. and Meth. in Phys. Res. B* **2007**, *258*, 352. **DOI:** 10.1016/j.nimb.2007.01.289
20. Simo, A.; Polte, J.; Pfänder, N.; Vainio, U.; Emmerling, F.; Rademann, K. *J. Am. Chem. Soc.* **2012**, *134*, 18824. **DOI:** 10.1021/ja309034n
21. Hosoya, Y.; Suga, T.; Yanagawa, T.; Kurokawa, Y. *J. Appl. Phys.* **1997**, *81*, 1475. **DOI:** 10.1063/1.363983
22. Manikandan, D.; Mohan, S.; Magudapathy, P.; Nair, K. G. M. *Physica B* **2003**, *325*, 86. **DOI:** 10.1016/S0921-4526(02)01453-9
23. Sole, J. G.; Bausa, L. E.; Jaque, D. *An Introduction to the Optical Spectroscopy of Inorganic Solids*, John Wiley & Sons, England, **2005**.
24. Al-Agel, F. A. *Vacuum* **2011,** *85*, 892. **DOI:** 10.1016/j.vacuum.2011.01.006
25. Wooten, F. *Optical Properties of Solids*, Academic Press, Inc., New York, **1972**.
26. Li, L.; Yang, Y.; Zhou, D.; Yang, Z.; Xu, X.; Qiu, J. *J. Appl. Phys.* **2013**, *113*, 193103. **DOI:** 10.1063/1.4807313
27. Jimenez, J. A.; Lysenko, S.; Zhang, G.; Liu, H. *J. Mater. Sci.* **2007,** *42*, 1856. **DOI:** 10.1007/s10853-006-0898-6
28. Garcia, M. A.; Garcia-Heras, M.; Cano, E.; Bastidas, J. M.; Villegas, M. A.; Montero, E.; Llopis, J.; Sada, C.; De Marchi, G.; Battaglin, G.; Mazzoldi, P. *J. Appl. Phys.* **2004,** *96*, 3737. **DOI:** 10.1063/1.1778473
29. Quaranta, A.; Rahman, A.; Mariotto, G.; Maurizio, C.; Trave, E.; Gonella, F.; Cattaruzza, E.; Gibaudo, E.; Broquin, J. E. *J. Phys. Chem. C* **2012**, *116*, 3757. **DOI:** 10.1021/jp2095399
30. Varma, R. S.; Kothari, D. C.; Tewari, R. *J. Non-Cryst. Solids* **2009**, *355*, 1246. **DOI:** 10.1016/j.jnoncrysol.2009.05.001